

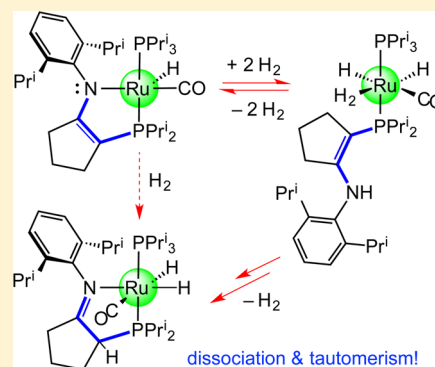
Ruthenium Complexes Stabilized by Bidentate Enamido-Phosphine Ligands: Aspects of Cooperative H₂ Activation

Truman C. Wambach and Michael D. Fryzuk*

Department of Chemistry, The University of British Columbia, 2036 Main Mall, Vancouver, British Columbia V6T 1Z1, Canada

Supporting Information

ABSTRACT: Four bidentate, hybrid ligands (^R(NP)^{R'}H) featuring imine-nitrogen and alkyl-phosphine donors linked by a cyclopentyl ring were synthesized. The ortho position of the aryl group attached to nitrogen is varied such that R is Me or Prⁱ; additionally, the groups decorating phosphorus (R') are varied between Bu^t or Prⁱ. The addition of each ligand to RuHCl(PPR₃)₂(CO) in the presence of KOBu^t generates four enamido-phosphine complexes RuH{^R(NP)^{R'}}(PPR₃)₂(CO) that were characterized by NMR spectroscopy, elemental analyses, and, in the case of R = Prⁱ and R' = Bu^t or Prⁱ, X-ray crystallography. Depending on R', the reaction of RuH{^R(NP)^{R'}}(PPR₃)₂(CO) with H₂ generates varying amounts of the imine-phosphine complex RuH_{2}{^R(NP)^{R'}H}(PPR₃)₂(CO). Insights into the mechanism of H₂ activation by these enamido derivatives were explored using RuH{^{Pr}(NP)^{Pr}}(PPR₃)₂(CO), for which an intermediate was identified as the dihydrogen–dihydride complex, RuH₂(H₂){^{Pr}(NP)^{Pr}H}(PPR₃)₂(CO), on the basis of the T_{1,min} value of 22 ms for the ¹H NMR resonance at δ -7.2 at 238 K (measured at 400 MHz). The N donor of the enamine tautomeric form of the ligand is protonated by H₂ or D₂ and dissociates from Ru. Tautomerization of the enamine to the imine form of the dissociated arm is involved in formation of the final product.}

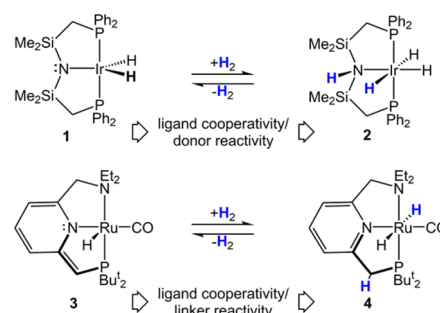


INTRODUCTION

Until recently, ligands were designed to be ancillary in nature, in other words, to remain innocent during any transformation at the metal center by providing the appropriate steric and electronic environment without getting involved in the actual process. However, ligand systems that can participate in reactions are a topic of current interest.^{1–5} A simple example of ligand-based reactivity is hemilability, which occurs when a donor of a multidentate ligand dissociates during a transformation to provide an open coordination site. Other examples are noninnocent or redox active ligands, wherein electrons can be stored on the ligand and are available for use by the complex. Of importance to this work are cooperative ligands that react in concert with a metal center to activate small molecules.¹

Scheme 1 depicts two specific types of ligand cooperativity that can be distinguished: donor reactivity^{6–8} and linker reactivity.^{9,10} In the iridium example, addition of dihydrogen to dihydride **1** results in the formation of the amine-trihydride **2** by heterolytic cleavage of H₂ across the iridium-amido unit, which we define as an example of donor reactivity. In the ruthenium example **3**, the heterolytic activation of H₂ also occurs, but in this case, a proton (H⁺) is transferred to the backbone of the ligand, and the hydride (H⁻) coordinates to the Ru(II) center in **4**. In both cases, H₂ is activated by the ligand and the metal center acting in a cooperative fashion, but the difference is which part of the ligand is protonated, the donor in **1** → **2**, or the linker in **3** → **4**. Other nomenclature has been developed to describe similar reactivity,⁴ and there are

Scheme 1



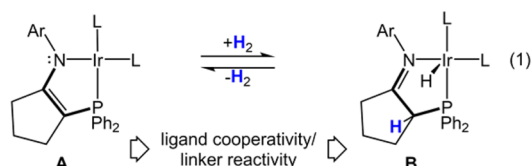
other types of ligand cooperativity that involve activation of small molecules at a remote site of the ligand, not necessarily the backbone of the ligand that links the different donors.^{11–14}

Linker reactivity is a key feature of the catalytic reactivity of numerous pyridine-based metal–ligand systems. For example, **3** and **4** are involved in the catalytic acceptorless dehydrogenation of primary alcohols to form esters¹⁵ and the reverse reaction, hydrogenation of esters to form primary alcohols.⁹ Numerous other pyridine-based linker reactive ligands are known,^{10,16–18} and coordination of this ligand architecture to a variety of late transition metals generates complexes that display linker reactivity. Importantly, in several cases, the enamido-phosphine unit (bolded in **3**, Scheme 1) cooperates with a metal, such that

Received: March 26, 2015

functionalization of the linker with a proton^{9,10,19,20} or other electrophile^{21–25} occurs without the formation of any observable intermediates. Computational evidence for select systems suggests that concerted proton transfer to the linker of the ligand occurs.^{20,26–30}

We recently reported our studies on replicating the linker reactivity shown for the transformation of **3** to **4**; however, instead of using the tridentate pyridine-based pincer ligand we focused our attention on a simplified, bidentate enamido-phosphine system, which is easily accessible by deprotonation of readily available imine-phosphine ligands. As shown in eq 1,



we discovered that the cyclopentyl-based enamido-phosphine derivative coordinated to Ir(I) (**A** in eq 1) could engage in processes that replicated the heterolytic cleavage of H₂ in a cooperative manner to generate **B**.³¹

While this iridium(I) system was found to add and release H₂, these systems did not catalyze the acceptorless dehydrogenation (AD) of alcohols due to the formation of a variety of stable, catalytically inactive iridium derivatives upon reaction with primary and secondary alcohols. In contrast to the ruthenium system in Scheme 1, the H₂ addition and loss resulted in a change in formal oxidation state at the metal center from Ir(I) to Ir(III) (**A** to **B**), and most importantly, H₂ loss (**B** to **A**) required addition of CO. What we also discovered was that the *N*-arylimine donor was prone to dissociation and putative enamine intermediates also did not bind to the iridium center during ligand induced H₂ loss.

We report here an update on our continued efforts to explore a simplified cooperative ligand that can replicate key aspects of the pyridine-based pincer ligands in Scheme 1. We also examine modifications of the same imine-phosphine scaffold with a Ru(II) precursor and its reactions with dihydrogen. What we have discovered is that while the final product appears to match linker reactivity in terms of product outcomes, the details of the process are more consistent with a stepwise transformation that involves a donor reactive pathway that is kinetically accessible followed by tautomerization to generate the final product.

SYNTHESIS OF RUTHENIUM ENAMIDO-PHOSPHINE COMPLEXES

The synthesis of cyclopentyl-linked imine phosphine ligands has been reported by us and others.^{31–34} In this work, the *ortho*

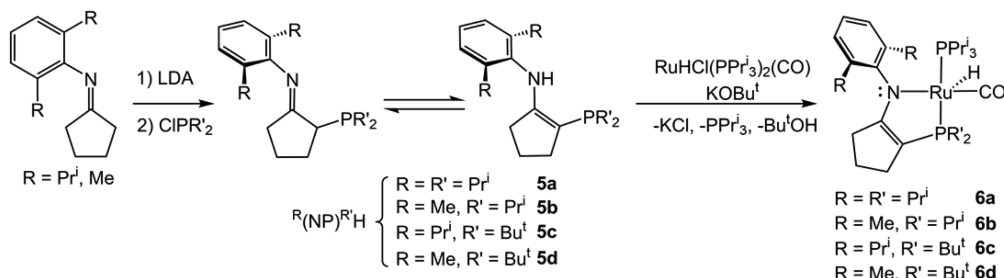
positions of the *N*-aryl group (R = Prⁱ or Me), and the substituents on the phosphine donor (R' = Prⁱ or Bu^t), are varied to explore the impact these modifications have on ligand cooperativity (Scheme 2). The short form descriptors of the ligands reported here are ^R(NP)^{R'}. In solution, the imine-phosphine and enamine-phosphine tautomers each display unique singlets in their ³¹P{¹H} NMR spectra, which allows easy determination of the amount of each tautomer. When R' is Prⁱ the equilibrium between the two tautomers slightly favors the enamine form over the imine tautomer. When R' is Bu^t the equilibrium is shifted almost entirely toward the enamine. The most sterically demanding ligand in this work is **5c**, and it exists exclusively as the enamine tautomer.

The reaction of **5a–d** with RuHCl(PPrⁱ₃)₂(CO) in the presence of 1 equiv of potassium *tert*-butoxide (KOBU^t) forms a dark red solution in every case. ³¹P{¹H} NMR spectroscopy shows two doublet resonances with large coupling constants indicative of trans disposed phosphines for the enamido-ruthenium complexes **6a–d**. After the reaction is complete and after workup, analytically pure complexes are obtained in acceptable yields (~42%). The multinuclear NMR spectra of **6a–d** are all consistent with C₁ symmetric, five-coordinate complexes.

When concentrated pentane solutions of **6a** or **6c** were cooled to –35 °C, crystals of both compounds were obtained and analyzed by X-ray diffraction. ORTEP representations of **6a** and **6c** are shown in Figures 1 and 2, respectively. For both **6a** and **6c**, the hydride ligand could be located and freely refined. Notably, both structures are distorted from an idealized geometry, but are approximately square pyramidal. For the PPrⁱ derivative, **6a**, the N1–Ru1–C32 bond angle is 155.36(5)°, and the corresponding angle in **6c** (N1–Ru1–C100) is more linear at 164.25(6)°, no doubt due to the large *tert*-butyl substituents on the latter. The H50–Ru1–C32 angle is 84.1(7)° for **6a**, and the corresponding angle in **6c** is 85(1)°. The above angles are noteworthy as DFT calculations performed on a related Ru enamido-phosphine complex, which could not be characterized by X-ray analysis, suggest that upon switching from an amido phosphine³⁵ to an enamido-phosphine donor a square-based pyramidal structure is favored over a trigonal bipyramidal geometry.²⁰ The structures of **6a** and **6c** are consistent with this proposal, as are the large, negative chemical shifts (ca. –24 ppm) of the hydride ligands of **6a** and **6c** observed by ¹H NMR spectroscopy.

The bond lengths and angles of the enamido-phosphine unit are nearly identical for both **6a** and **6c**; however, some subtle differences occur in the bond lengths around the coordination sphere of the two ruthenium centers. The Ru1–N1 bond length is slightly longer for the PBU^t derivative; for example, for

Scheme 2



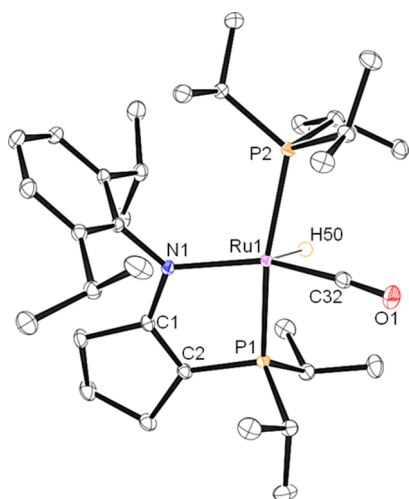


Figure 1. ORTEP drawing of the solid-state molecular structure of **6a** with probability ellipsoids at 50%. Hydrogen atoms are omitted for clarity, with the exception of H50, which was found in the difference map. Selected bond lengths (Å) and angles (deg): Ru1–N1 2.1287(2), Ru1–P1 2.3273(6), Ru1–P2 2.4081(6), Ru1–C32 1.8196(2), N1–C1 1.3796(2), C1–C2 1.3643(2), C2–P1 1.7629(2), C32–O1 1.1640(2), N1–C1–C2 125.42(2), C1–C2–P1 113.52(2), N1–Ru1–P1 81.47(4), C32–Ru1–P1 88.62(5), N1–Ru1–P2 106.42(4), P1–Ru1–P2 166.600(2), N1–Ru1–C32 155.36(5), C32–Ru1–H50 84.1(7).

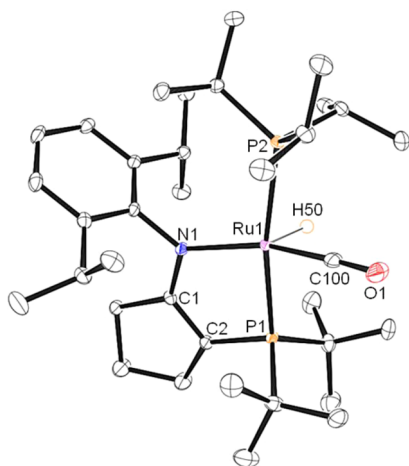


Figure 2. ORTEP drawing of the solid-state molecular structure of **6c** with probability ellipsoids at 50%. Hydrogen atoms are omitted for clarity, with the exception of H50, which was found in the difference map. Selected bond lengths (Å) and angles (deg): Ru1–N1 2.1427(2), Ru1–P1 2.3576(4), Ru1–P2 2.4217(4), Ru1–C100 1.8228(2), N1–C1 1.3774(2), C1–C2 1.372(2), C2–P1 1.7703(2), C100–O1 1.169(2), N1–C1–C2 125.24(2), C1–C2–P1 113.94(1), N1–Ru1–P1 81.05(3), C100–Ru1–P1 90.21(5), N1–Ru1–P2 106.19(3), P1–Ru1–P2 169.060(2), N1–Ru1–C100 164.25(6), C100–Ru1–H50 85(1).

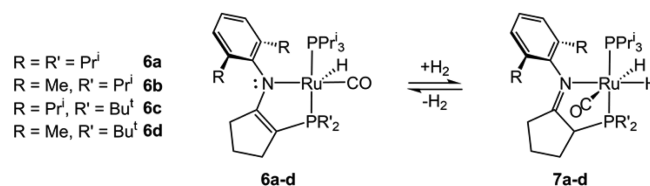
6a this bond distance is 2.1287(2) Å, and lengthens to 2.1427(2) Å for **6c**. The oxygen–carbon bond length of the carbonyl group attached to ruthenium is 1.1641(2) Å for **6a** and 1.169(2) Å for **6c**; therefore, changing from PPr₂ to PBu^t₂ groups has little influence on the length of the CO triple bond of the carbonyl ligand. The CO stretching frequencies of **6a–d** are very similar and range from 1893 to 1899 cm⁻¹ (see Supporting Information, Table S1), which indicates that the difference in electronic influence of these ligands on Ru is

minimal, as reflected by the CO ligand. Interestingly, the CO stretch for **3** is also 1899 cm⁻¹, which is virtually identical to the series of derivatives reported here. Given the differences in H₂ activation for complexes **6a–d** as compared to each other and to **3**, it is clear that electronic effects at ruthenium are apparently not that important for cooperative H₂ activation for **6a–d**.

REACTIVITY OF RUTHENIUM ENAMIDO-PHOSPHINE COMPLEXES WITH DIHYDROGEN

As monitored by ¹H, ¹H{³¹P}, and ³¹P{¹H} NMR spectroscopy, exposing solutions of **6a–d** to 1–4 atm of H₂ forms products consistent with **7a–d** (Scheme 3).

Scheme 3



Carefully controlling hydrogen pressure, solvent volume, and headspace volume allows addition of reproducible amounts of dihydrogen to samples of **6a–d**, which allows the effects of changing the sterics of the ligands on the H₂ addition process to be ascertained. The least sterically demanding variant (**6b**) proceeds to completion with H₂ to form two products in a 2.4:1.0 ratio. The two products likely correspond to diastereomers due to the presence of the chiral center on the ligand and the chiral ruthenium center; that is, the α-CH unit can be *syn* or *anti* to the carbonyl ligand. The presence of these two diastereomers for **7b** complicates the solution ¹H NMR data enough that assignment of the resonances for the minor diastereomer was not attempted. Importantly, ¹H–¹³C HSQC allows for assignment of ¹³C resonances as α-CH protons for both the major and minor isomer; therefore, the imine tautomeric form of the ligand is bound to Ru in both cases (see Supporting Information). A major and minor diastereomer also form when **6d** reacts with H₂. Trace resonances in the ¹H NMR spectra of **7a** and **7c** are consistent with small amounts of a second diastereomer. The selectivity for one diastereomer over the other is apparently governed by the sterics on the N-aryl moiety, as only small amounts of a second diastereomer appear in the ¹H NMR spectra of **7a** and **7c**, which have the bulkier ortho-isopropyl substituents.

When the alkyl groups decorating phosphorus (R') are changed from isopropyl to *tert*-butyl, the rate of dihydrogen addition is much slower, and the reactions never reach completion despite an observable (by ¹H NMR spectroscopy) excess of H₂ and extended reaction times. Identification of **7c,d** is based on ¹H NMR resonances consistent with the hydride ligands observed for complexes **7a,b**; the low concentrations of **7c,d** relative to the respective starting materials are such that obtaining ¹³C NMR data was not attempted and no further characterization was possible.

The reaction of **6a** with H₂ proceeds to completion over the course of approximately 12 h at room temperature. The resulting complex **7a** is isolated as a pale yellow, crystalline solid after workup, in one diastereomeric form. In the ³¹P{¹H} NMR spectrum of **7a**, new resonances at δ 74.5 and 92.9 are

observed, with a P–P coupling constant ($^2J_{PP} = 252.3$ Hz) that is consistent with *trans* disposition of the two phosphine ligands. Two signals in the hydride region of the ^1H NMR spectrum at $\delta -18.4$ and -5.5 are observed. Additionally, a resonance assigned to the α -CH proton that results from the overall heterolytic cleavage of H_2 at $\delta 3.1$ can be identified. Multinuclear NMR studies as well as deuterium labeling experiments confirm that the linker α -CH of **7a** originates from added H_2 .

Dissolving **7a** in a minimal amount of pentane and cooling the mixture to -35 °C resulted in formation of X-ray quality crystals. Figure 3 shows an ORTEP representation of **7a**. The

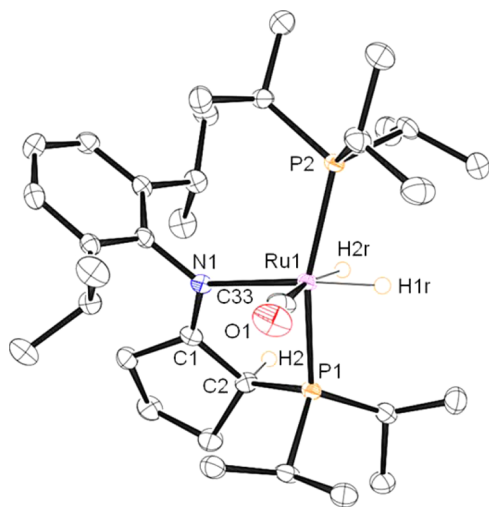
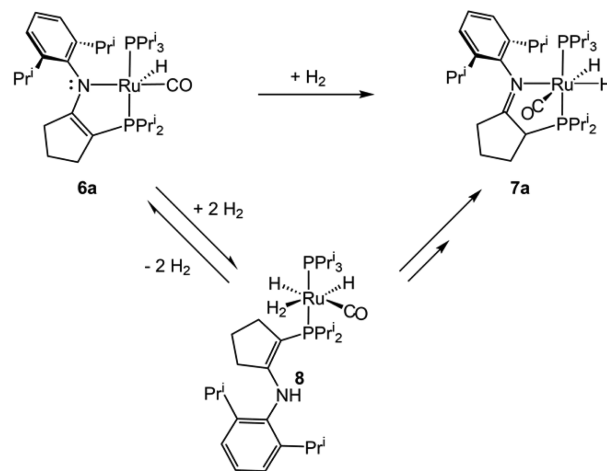


Figure 3. ORTEP drawing of the solid-state molecular structure of **7a** with probability ellipsoids at 50%. All of the hydrogen atoms except α -CH proton and hydrides are omitted for clarity. The α -CH proton and hydrides were located in the difference map. Selected bond lengths (Å) and angles (deg): Ru1–N1 2.306(3), Ru1–P1 2.2923(2), Ru1–P2 2.3310(2), Ru1–C32 1.872(6), N1–C1 1.293(6), C1–C2 1.510(6), C2–P1 1.854(5), C32–O1 1.172(6), N1–C1–C2 122.3(4), C1–C2–P1 109.1(3), N1–Ru1–P1 80.82(9), C33–Ru1–P1 100.50(2), N1–Ru1–P2 107.77(9), P1–Ru1–P2 161.99(4), N1–Ru1–C33 101.33(2).

ruthenium center is bound to two hydride ligands that are *cis* disposed to one another. The α -CH proton of the ligand is disposed *anti* to the carbonyl moiety. Interestingly, another molecule corresponding to **7a** is present in the asymmetric unit of the crystal structure. Both molecules in the asymmetric unit feature the *S* enantiomer of the imine-phosphine ligand coordinated to ruthenium. The other enantiomer of **7a**, with the *R* form of the ligand coordinated to ruthenium, is also present in the crystal lattice; the *c*-glide plane of the space group ($P2_1/c$) generates it. Overall, the most notable feature of the solid-state structure is the *cis* disposition of the two hydride ligands. In comparison, *trans* hydrides are observed for the pyridine-based pincer ligated ruthenium complex (**4**) and related compounds (Scheme 1).^{9,10,20,36,37} As will be discussed below, this change in the relative disposition of the hydrides was the first clue that the mechanism of H_2 addition is different for our system in comparison to **3**.

Monitoring the conversion of **6a** to **7a** under approximately 3.6 atm (6.5 equiv) of dihydrogen by ^1H and $^{31}\text{P}\{^1\text{H}\}$ NMR spectroscopy revealed that an intermediate species, **8**, forms after less than 20 min and goes on to form **7a** (Scheme 4) over a period of 5.4 h (95% complete). While this intermediate was

Scheme 4



never isolated as a pure material, several spectroscopic features are consistent with the dihydrogen dihydride complex (**8**) shown in Scheme 4.

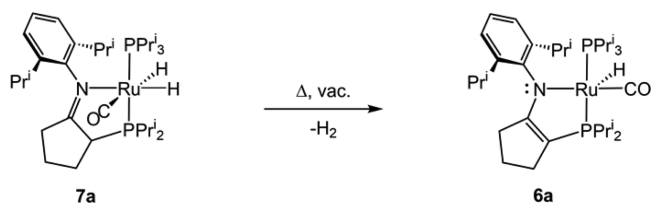
Doublet resonances at $\delta 80.1$ and 41.2 assigned to **8** are observed by $^{31}\text{P}\{^1\text{H}\}$ NMR spectroscopy. The P–P coupling constant ($^2J_{PP} = 195.8$ Hz) confirms that the phosphine ligands remain *trans* to one another. Certain resonances in the ^1H NMR spectrum are especially diagnostic. For example, a sharp singlet at $\delta 8.9$ is assigned as the N–H proton of **8**. A broad resonance at $\delta -7.2$ that integrates to four protons relative to the signal at $\delta 8.9$ is also observed. Measuring the relaxation time of this upfield resonance at 400 MHz in a solution of 5% CH_2Cl_2 in d_8 -toluene as a function of temperature gives a $T_{1,\text{min}}$ value of 22 ms at 238 K. This relaxation time is comparable to $T_{1,\text{min}}$ values reported for two similar dihydrogen dihydride complexes: $\text{RuH}_2(\text{H}_2)(\text{CO})(\text{PPr}^i_3)_2$ ($T_{1,\text{min}} = 15$ ms at 200 K, measured at 200 MHz)³⁸ and $\text{RuH}_2(\text{H}_2)(\text{CO})(\text{PCp}_3)_2$ ($T_{1,\text{min}} = 42$ ms at 233 K measured at 500 MHz).³⁹ The abbreviation PCp_3 in this case corresponds to tricyclopentylphosphine.

Despite several attempts, decoalescence of the hydride ligands from the dihydrogen ligand was never observed using the conditions employed. Complete disappearance of the dihydrogen–dihydride signal occurred at temperatures below 213 K, and the lowest temperature at which meaningful spectra could be recorded was 173 K. Further cooling to 153 K did not give any return of signal intensity, and very broad ^1H NMR resonances were observed, possibly due to freezing of the solvent.

Deuterium labeling studies support the assignment of **8** as a dihydrogen dihydride complex. For instance, exposing **6a** to D_2 shows rapid deuterium scrambling into the broad resonance at $\delta -7.2$ corresponding to **8**. This is consistent with a highly fluxional dihydrogen–dihydride species.^{38–41} A key feature of **8** is the protonated enamine that is dissociated from the ruthenium center, wherein the N–H proton results from added H_2 . Consistent with this proposal, the resonance at $\delta 8.9$ is not observed when D_2 gas is used in place of H_2 (see Supporting Information). An additional observation made during these experiments is the ^1H NMR resonance that corresponds to the hydride ligand of the starting material **6a** disappears much more quickly than the other diagnostic resonances of **6a**. This suggests that **6a** and **8** are in equilibrium since the hydride of **6a** exchanges for a deuteride under D_2 .

The reverse reaction (Scheme 5), the loss of H₂ from **7a** to form **6a**, occurs slowly at room temperature under an

Scheme 5

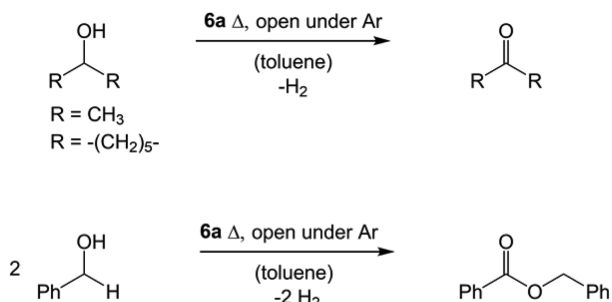


atmosphere of nitrogen. Evacuating the headspace of a J. Young NMR tube containing a solution of **7a**, and heating this mixture to 60 °C, gives full conversion of **7a** to **6a** overnight. Unfortunately, no intermediates were detected by ³¹P{¹H} or ¹H NMR spectroscopy. Monitoring H₂ loss as a function of time shows only resonances for the dihydride starting material **7a** and the enamido-phosphine hydride product **6a**, although signals of the latter are broadened, presumably due to some reactivity with hydrogen that is released into the headspace of the NMR tube.

EFFORTS TOWARD CATALYTIC DEHYDROGENATION OF ALCOHOLS

Having established the ability of these complexes to reversibly add and release H₂, attempts to apply this reactivity to the catalytic acceptorless dehydrogenation (AD) of isopropanol, cyclohexanol, and/or benzyl alcohol (Scheme 6) were made.

Scheme 6



These efforts show certain processes inhibit formation of an active catalyst. Initially, **6a** was found to be thermally unstable under catalytic conditions at temperatures >110 °C, which are normally used for alcohol dehydrogenation reactivity (Table 1).¹⁰ For example, heating **6a** in refluxing toluene with isopropanol, or cyclohexanol under Ar vented to a mercury

bubbler, gave no catalytic turnover. Analysis of the reaction mixture by ³¹P{¹H} NMR spectroscopy showed free PPr₃, consistent with decomposition. Lowering the temperature to 60 °C allowed for catalytic dehydrogenation of isopropanol and cyclohexanol (Table 1, entries 2 and 4). Monitoring 0.9 turnovers of AD converting isopropanol to acetone in an evacuated J. Young tube by ¹H NMR spectroscopy shows hydride resonances that are consistent with **7a**. The relative concentrations of **6a** and **7a** vary somewhat during AD; however, full conversion to **7a** was not observed. The ratio of **6a**:**7a** is approximately 1:1.2 after 0.9 turnovers, suggesting **7a** can release H₂ under these conditions.

Attempts to dehydrogenate benzyl alcohol to benzyl benzoate at 60 °C under similar conditions to those used for secondary alcohol dehydrogenation were unsuccessful. Initial attempts gave ~1% conversion to benzyl benzoate. Recorded ³¹P{¹H} NMR spectra of the reaction mixture prior to heating show release of PPr₃ and formation of a variety of products. Addition of 1 equiv of pyridine relative to ruthenium had little effect on the catalytic performance (~2% conversion); likewise, addition of 1 equiv of PMe₃ to **6a** had little effect (~3% conversion).

CONCLUSION

The synthesis and reactivity of a series of bidentate enamido-phosphine ligands coordinated to ruthenium extend the linker reactivity previously reported for **3** and related compounds^{9,10,20,36} to new systems. Variation of the groups decorating the N and P donor atoms of the bidentate ligands explored here shows that the sterics of the phosphorus donor have a profound impact on the reactivity of **6a–d** with H₂. The reactivity of **6a** with H₂ is reversible, a potentially important feature of an AD catalyst. Monitoring the reactivity of **6a** with primary and secondary alcohols demonstrates that it is a catalyst precursor for secondary alcohol dehydrogenation. Attempts to use **6a** as AD catalysts for benzyl alcohol dehydrogenation were unsuccessful, likely due to the thermal instability of putative intermediates, such as **8**. Perhaps the most intriguing feature of these studies is the reactivity of **6a** with H₂. Identification of dihydrogen–dihydride **8** as an intermediate, which forms during conversion of **6a** to **7a**, demonstrates that N-donor dissociation and tautomerization of the dissociated arm of the ligand between enamine and imine forms are involved in linker reactivity for this system. The mechanism for linker reactivity described in this Article is a unique alternative to what is commonly reported for other tridentate and tetradentate metal–ligand systems, where linker reactivity occurs via a concerted mechanism.

Table 1. Reactivity Studies

entry	catalyst	time (h)	temp (°C)	substrate	product	TON ^a	TOF (h ⁻¹)
1	6a	12	115	2-propanol			
2	6a	12	60	2-propanol	acetone	100	8.3
3	6a	12	115	cyclohexanol		0	
4	6a	12	60	cyclohexanol	cyclohexanone	50	7
5	6a	16	60	benzylalcohol	benzylbenzoate	~1	
6	6a ^b	16	60	benzylalcohol	benzylbenzoate	~2	
7	6a ^c	16	60	benzylalcohol	benzylbenzoate	~3	

^aCalculated by dividing moles of desired product by moles of **6a**. ^b1 equiv of pyridine was added to **6a** prior to addition of substrate and heating. ^c1 equiv of PMe₃ was added to **6a** prior to addition of substrate and heating.

EXPERIMENTAL SECTION

All procedures and manipulations were performed under an atmosphere of dry, oxygen-free dinitrogen or argon by means of standard Schlenk or glovebox techniques. Argon and dinitrogen were dried and deoxygenated by passing the gases through a column containing molecular sieves and a Cu catalyst. Dihydrogen and was dried by passage through activated molecular sieves prior to use. D₂ and ¹³C gas were purchased from Cambridge Isotope Laboratories and used as received. Hexanes, toluene, THF, and diethyl ether were purchased from Aldrich, dried by passage through a tower of alumina, and degassed by passage through a tower of Q-5 catalyst under positive pressure of nitrogen. Pentane was dried using Na/K and benzophenone and collected from a solvent still. Deuterated toluene and benzene were dried over NaK/benzophenone, trap-to-trap distilled, and freeze–pump–thaw degassed three times. Potassium *tert*-butoxide was purchased and purified by sublimation. Isopropanol, cyclohexanol, and benzylalcohol were dried over sodium, then distilled into a Kontes sealed flask and freeze–pump–thaw degassed. Diisopropyl amine was distilled and freeze–pump–thaw degassed. Cyclopentanone, 2,6-dimethylaniline, 2,6-diisopropylaniline, and *n*-butyl lithium were purchased and used as received. RuCl₃ hydrate was purchased from Pressure Chemical Company and used as received. RuHCl(PPPr₃)₂(CO)⁴² was synthesized by a literature procedure. ATR (attenuated total reflectance) FTIR (Fourier transform infrared spectroscopy) spectra were recorded on a PerkinElmer Frontier FTIR spectrometer. NMR (nuclear magnetic resonance) spectra were recorded on Bruker Avance II 300 MHz or Bruker Avance 400 MHz spectrometers unless otherwise noted. Chemical shifts for ³¹P nuclei were referenced to 85% H₃PO₄ in H₂O (0 ppm). ¹H nuclei were referenced to resonances of the residual protonated solvents relative to tetramethylsilane (0 ppm), and ¹³C spectra were referenced to the solvent carbon resonance(s). Elemental analysis was performed at the facilities of the Chemistry Department of the University of British Columbia. Gas chromatography–mass spectrometry (GC–MS) analyses were performed on an Agilent 6890N instrument using an Agilent HP-5MS column (30 m length, 0.25 mm diameter, 0.25 μm film). Quantitative ¹H NMR spectra recorded using 1,3,5-trimethoxybenzene as an internal standard were recorded using a relaxation delay time (d1) of 57 s. **Caution!** All reactions that resulted in a pressure of 1.5 atm or greater within a sealed vessel upon warming to room temperature were performed with great care, and always manipulated behind a blast shield. Pressurized NMR tubes were allowed to warm to room temperature in a safe location and used with caution; protective eye wear was worn at all times.

General Procedure for the Synthesis of RuH^(Me)(NP)^{Pri}(PPPr₃)₃(CO) (6a), RuH^(Me)(NP)^{Pri}(PPPr₃)₃(CO) (6b), RuH^(Pri)(NP)^{Bu}(PPPr₃)₃(CO) (6c), and RuH^(Me)(NP)^{Bu}(PPPr₃)₃(CO) (6d). The appropriate imine-phosphine ligand (0.411 mmol) was combined with RuHCl(PPPr₃)₂(CO) (0.200 g, 0.411 mmol) and potassium *tert*-butoxide (0.046 g, 0.411 mmol) in a vial fitted with a stir bar in the glovebox. THF (5 mL) was added, which immediately produced a dark red color indicative of formation of the desired product. The reaction mixture was stirred for approximately 4 h and monitored by ³¹P{¹H} NMR spectroscopy until complete, whereupon the mixture was taken to dryness and the residue was dissolved in a minimal amount of pentane (~5 mL). The pentane solution was filtered through Celite into a small round-bottom flask, and the pentane and free PPr₃ were removed under vacuum. The crude product was dissolved in a minimal amount of pentane, and upon cooling to –35 °C overnight analytically pure crystalline samples of each complex were obtained.

RuH^(Pri)(NP)^{Pri}(PPPr₃)₃(CO) (6a). (Yield after recrystallization: 0.097 g, 36%.) ³¹P{¹H} NMR (C₆D₆, 161.9 MHz, 298 K): δ 39.5 (d, ²J_{PP} = 245.2 Hz, 1P, Ru–PPPr₃), 59.8 (d, ²J_{PP} = 245.2 Hz, 1P, Ru–P_{ligand}). ¹H NMR (C₆D₆, 400 MHz, 298 K): δ –23.3 (dd, ²J_{PH} = 18.6 Hz, ²J_{PH} = 22.1 Hz, 1H, Ru–H), 0.83 (dd, ³J_{HH} = 7.2 Hz, ³J_{PH} = 11.9 Hz, 9H, P–PrⁱCH₃), 1.1–1.3(4) (m, 34H (30H expected, trace PPr₃ may explain slight over integration), N/P–PrⁱCH₃), 1.5 (dd, ³J_{HH} = 7.0 Hz, ³J_{PC} = 16.9 Hz, 3H, P–PrⁱCH₃), 1.7 (m, 1H, β-CH₂), 2.0 (m, 1H, β-CH₂), 2.1 (m, 4H, 3× P–PrⁱCH/γ-CH₂), 2.2 (m, 2H, P–PrⁱCH, γ-CH₂), 2.3 (m, 1H, δ-CH₂), 2.5 (m, 1H, δ-CH₂), 2.7 (d, sept, ²J_{PH} = 4.4 Hz, ³J_{HH}

= 6.6 Hz, 1H, P–PrⁱCH), 3.4 (sept, ³J_{HH} = 6.9 Hz, 1H, N–PrⁱCH), 3.5 (sept, ³J_{HH} = 6.7 Hz, 1H, N–PrⁱCH), 7.1 (m, 3H, N–ArCH). ¹³C APT NMR (C₆D₆, 100.6 MHz, 298 K): δ 18.1 (d, ³J_{PC} = 3.5 Hz, P–PrⁱCH₃), 18.5(s) (d, ³J_{PC} = 2.4 Hz, P–PrⁱCH₃), 18.6 (d, ²J_{PC} = 2.4 Hz, P–PrⁱCH₃), 18.7 (s, P–PrⁱCH₃), 19.6 (d, ³J_{PC} = 4.0 Hz, P–PrⁱCH₃), 20.1 (s, P–PrⁱCH₃), 23.0 (s, N–PrⁱCH₃), 23.3 (s, N–PrⁱCH₃), 23.5 (d, ³J_{PC} = 28.9 Hz, P–PrⁱCH), 24.0 (s, N–PrⁱCH₃), 25.1 (d, ³J_{PC} = 27.1 Hz, P–PrⁱCH), 25.2 (s, N–PrⁱCH₃), 26.0 (dd, ³J_{PC} = 1.9 Hz, ¹J_{PC} = 14.8 Hz, P–PrⁱCH), 28.2 (s, N–PrⁱCH), 28.7 (s, N–PrⁱCH), 28.8 (d, ³J_{PC} = 6.2 Hz, γ-CH₂), 29.5 (m, δ-CH₂), 33.1 (d, ³J_{PC} = 16.6 Hz, β-CH₂), 84.4 (d, ¹J_{PC} = 41.6 Hz, α-C), 122.6 (s, N–*p*-ArCH), 123.4 (s, N–*m*-ArCH), 124.3 (s, N–*m*-ArCH), 142.8 (s, N–ArCPrⁱ), 143.3 (s, N–ArCPrⁱ), 156.4 (s, N–CAr), 187.5 (dd, ³J_{PC} = 4.3 Hz, ²J_{PC} = 33.3 Hz, N–C_{enamido}), 207.3 (v t, ²J_{PC} = 14.9 Hz, Ru–CO). ATR-FTIR νCO (cm^{–1}): 1899. Anal. Calcd for C₃₃H₅₉NOP₂Ru: C, 61.09; H, 9.17; N, 2.16. Found: C, 61.19, H, 9.45, N, 2.11.

RuH^(Me)(NP)^{Pri}(PPPr₃)₃(CO) (6b). (Yield after recrystallization: 0.063 g, 26%.) ³¹P{¹H} NMR (C₆D₆, 161.9 MHz, 298 K): δ 47.4 (d, ²J_{PP} = 243.9 Hz, 1P, Ru–PPPr₃), 59.1 (d, ²J_{PP} = 243.9 Hz, 1P, Ru–P_{ligand}). ¹H NMR (C₆D₆, 400 MHz, 298 K): δ –25 (dd, ²J_{PH} = 18.0 Hz, ²J_{PH} = 20.5 Hz, 1H, Ru–H), 0.97 (dd, ³J_{HH} = 7.2 Hz, ³J_{PH} = 12.4 Hz, 9H, P–PrⁱCH₃), 1.1 (dd, ²J_{HH} = 7.1 Hz, ²J_{PH} = 12.7 Hz, 9H, P–PrⁱCH₃), 1.1(6) (dd, ³J_{HH} = 6.0 Hz, ³J_{PC} = 10.8 Hz, 3H, P–PrⁱCH₃), 1.2(2) (dd, ²J_{HH} = 6.9 Hz, ³J_{PH} = 15.9 Hz, 3H, P–PrⁱCH₃), 1.3 (dd, ³J_{HH} = 6.9 Hz, ³J_{PH} = 15.7 Hz, 3H, P–PrⁱCH₃), 1.4 (dd, ³J_{HH} = 7.0 Hz, ³J_{PH} = 16.6 Hz, 3H, P–PrⁱCH₃), 1.7 (dq, ³J_{HH} = 6.8 Hz, ³J_{PH} = 13.4 Hz, 3H, P–PrⁱCH), 1.9 (m, 2H, β-CH₂), 2.1 (m, 3H, γ-CH₂/P–PrⁱCH), 2.2 (s, 3H, N–CH₃), 2.3 (s, 3H, N–CH₃), 2.3(s) (m, 1H, δ-CH₂), 2.4 (m, 1H, δ-CH₂), 2.7 (m, 1H, P–PrⁱCH), 6.7 (v dd, ³J_{HH} = 7.2 Hz, ³J_{HH} = 7.6 Hz, 1H, N–*p*-ArCH), 7.0 (v d, J = 7.4 Hz, 2H, N–*m*-ArCH). ¹³C APT NMR (C₆D₆, 100.6 MHz, 298 K): δ 18.3 (d, ³J_{PC} = 3.2 Hz, P–PrⁱCH₃), 18.8 (d, ³J_{PC} = 5.3 Hz, 2× P–PrⁱCH₃), 19.4 (d, ²J_{PC} = 4.0 Hz, P–PrⁱCH₃), 19.9 (s, P–PrⁱCH₃), 20.0 (s, N–CH₃), 20.1 (s, N–CH₃), 20.6 (s, P–PrⁱCH₃), 23.2 (d, ¹J_{PC} = 31.9 Hz, P–PrⁱCH), 25.5 (s, P–PrⁱCH), 25.6 (dd, ³J_{PC} = 2.1, ¹J_{PC} = 15.2 Hz, P–PrⁱCH), 28.7 (d, ³J_{PC} = 6.4 Hz, δ-CH₂), 29.7 (br s, γ-CH₂), 31.4 (d, ²J_{PC} = 16.7 Hz, β-CH₂), 84.7 (d, ¹J_{PC} = 41.2 Hz, α-C), 123.2 (s, N–*p*-ArCH), 127.5 (s, N–*m*-ArCH), 127.7 (s, N–*m*-ArCH), 135 (s, N–ArCMe), 135.0 (s, N–ArCMe), 157.9 (s, N–CAr), 185.7 (dd, ³J_{PC} = 5 Hz, ²J_{PC} = 33.3 Hz, N–C_{enamido}), 207.0 (dd, ³J_{PC} = 15.4 Hz, ²J_{PC} = 25.1 Hz, Ru–CO). ATR-FTIR νCO (cm^{–1}): 1894. Anal. Calcd for C₂₉H₅₁NOP₂Ru: C, 58.76; H, 8.67; N, 2.36. Found: C, 58.73, H, 8.64, N, 2.37.

RuH^(Pri)(NP)^{Bu}(PPPr₃)₃(CO) (6c). (Yield after recrystallization: 0.153 g, 55%.) ³¹P{¹H} NMR (C₆D₆, 161.9 MHz, 298 K): δ 39.5 (d, ²J_{PP} = 245.7 Hz, 1P, Ru–PPPr₃), 73.2 (d, ²J_{PP} = 245.7 Hz, 1P, Ru–P_{ligand}). ¹H NMR (C₆D₆, 400 MHz, 298 K): δ –24.0 (dd, ²J_{PH} = 18.8 Hz, ²J_{PH} = 20.2 Hz, 1H, Ru–H), 0.9 (dd, ³J_{HH} = 7.2 Hz, ³J_{PC} = 12.1 Hz, 9H, P–PrⁱCH₃), 1.1 (m, 12H, N/P–PrⁱCH₃), 1.2 (d, ³J_{HH} = 6.7 Hz, 3H, N–PrⁱCH₃), 1.2(8) (d, ³J_{HH} = 6.7 Hz, 3H, N–PrⁱCH₃), 1.2(9) (d, ³J_{HH} = 6.9 Hz, 3H, N–PrⁱCH₃), 1.5 (d, ³J_{PH} = 13.1 Hz, 9H, P–Bu^tCH₃), 1.6 (d, ³J_{PH} = 12.9 Hz, 9H, P–Bu^tCH₃), 1.7 (m, 1H, β-CH₂), 1.8(9) (m, 1H, β-CH₂), 2.0 (m, 2H, γ-CH₂), 2.1 (m, 3H, P–PrⁱCH), 2.5 (m, 1H, δ-CH₂), 2.7 (m, 1H, δ-CH₂), 3.4 (sept, ³J_{HH} = 6.9 Hz, 1H, N–PrⁱCH), 3.6 (sept, ³J_{HH} = 6.7 Hz, 1H, N–PrⁱCH), 7.1 (br s, 3H, N–ArCH). ¹³C APT NMR (C₆D₆, 100.6 MHz, 298 K): δ 18.9 (s, P–PrⁱCH₃), 20.0 (s, P–PrⁱCH₃), 23.4 (s, N–PrⁱCH₃), 23.9 (s, N–PrⁱCH₃), 25 (s, N–PrⁱCH₃), 25.0 (s, N–PrⁱCH₃), 25.7 (d, ³J_{PC} = 1.8 Hz, ¹J_{PC} = 15.2 Hz, P–PrⁱCH), 28.3 (s, N–PrⁱCH), 28.4(7) (s, N–PrⁱCH), 28.5 (m, γ-CH₂), 30.3(s) (d, ²J_{PC} = 3.8 Hz, P–Bu^tCH₃), 30.4 (d, ²J_{PC} = 4.4 Hz, P–Bu^tCH₃), 32.3 (m, δ-CH₂), 33.5 (d, ²J_{PC} = 16.4 Hz, β-CH₂), 36.0 (d, ¹J_{PC} = 23.7 Hz, P–Bu^tC), 40.9 (d, ¹J_{PC} = 20.6 Hz, P–Bu^tC), 86.7 (d, ¹J_{PC} = 38.4 Hz, α-C), 122.9 (s, N–*m*-ArCH), 123.3 (s, N–*m*-ArCH), 124.3 (s, N–*p*-ArCH), 143.1 (s, N–ArCPrⁱ), 143.6 (N–ArCPrⁱ), 156.6 (N–CAr), 186.7 (dd, ³J_{PC} = 4.5 Hz, ²J_{PC} = 33.0 Hz, N–C_{enamido}), Ru–CO not observed. ATR-FTIR νCO (cm^{–1}): 1893. Anal. Calcd for C₃₅H₆₃NOP₂Ru: C, 62.10; H, 9.38; N, 2.07. Found: C, 61.93, H, 9.61, N, 2.04.

RuH^(Me)(NP)^{Bu}(PPPr₃)₃(CO) (6d). (Yield after recrystallization: 0.215 g, 55%.) ³¹P{¹H} NMR (C₆D₆, 161.9 MHz, 298 K): δ 46.5 (d, ²J_{PP} = 242.6 Hz, 1P, Ru–PPPr₃), 72.4 (d, ²J_{PP} = 242.6 Hz, 1P, Ru–P_{ligand}). ¹H

NMR (C_6D_6 , 400 MHz, 298 K): δ -24.8 (dd, $^2J_{PP} = 18.0$ Hz, $^2J_{PP} = 18.8$ Hz, 1H, Ru-H), 1.0 (dd, $^3J_{HH} = 7.2$ Hz, $^3J_{PH} = 12.7$ Hz, 9H, P-PrⁱCH₃), 1.1 (dd, $^3J_{HH} = 7.2$ Hz, $^3J_{PH} = 12.5$ Hz, 9H, P-PrⁱCH₃), 1.5 (d, $^3J_{PH} = 13.2$ Hz, 9H, P-Bu^tCH₃), 1.5(1) (d, $^3J_{PH} = 12.8$ Hz, 9H, P-Bu^tCH₃), 1.7 (m, 3H, P-PrⁱCH), 1.8 (v t, $J = 2.2$ Hz, 2H, β -CH₂), 2.1 (m, 2H, γ -CH₂), 2.2 (s, 3H, N-CH₃), 2.4 (s, 3H, N-CH₃), 2.5 (m, 1H, δ -CH₂), 2.6 (m, 1H, δ -CH₂), 6.9 (t, $^3J_{HH} = 6.9$ Hz, 1H, N-*p*-ArCH), 7.0 (v d, $^3J_{HH} = 7.4$ Hz, 2H, N-*m*-ArCH). ¹³C APT NMR (C_6D_6 , 100.6 MHz, 298 K): δ 20.0 (s, P-PrⁱCH₃), 20.2 (s, P-PrⁱCH₃), 20.3 (s, 2 \times N-CH₃), 25.0 (dd, $^4J_{PC} = 1.8$ Hz, $^1J_{PC} = 15.5$ Hz, P-PrⁱCH), 28.8 (d, $^3J_{PC} = 6.0$ Hz, γ -CH₂), 30.1 (v t, $^2J_{PC} = 3.8$ Hz, 2 \times P-Bu^tCH₃), 31.8 (d, $^2J_{PC} = 16.4$ Hz, β -CH₂), 32.4 (v t, $J_{PC} = 1.9$ Hz, δ -CH₂), 35.2 (dd, $^3J_{PC} = 1.3$ Hz, $^1J_{PC} = 22.9$ Hz, P-CBu^t), 42.2 (d, $^1J_{PC} = 21.0$ Hz, P-CBu^t), 86.5 (d, $^1J_{PC} = 39.4$ Hz, α -C), 123.1 (s, N-*p*-ArCH), 127.7 (s, 2 \times N-*m*-ArCH), 134.2 (s, N-ArCMe), 135.4 (s, N-ArCMe), 158.0 (s, N-Car), 184.5 (dd, $^3J_{PC} = 4.0$ Hz, $^2J_{PC} = 32.4$ Hz, N-C_{enamide}), 207.2 (dd, $^2J_{PC} = 13.7$ Hz, $^2J_{PC} = 15.2$ Hz, Ru-CO). ATR-FTIR ν CO (cm⁻¹): 1895. Anal. Calcd for C₃₃H₅₅NOP₂Ru: C, 59.98; H, 8.93; N, 2.26. Found: C, 59.99; H, 9.06; N, 2.51.

Synthesis of RuH₂^{[P^{ri}(NP)^{PrⁱH}](PP^r₃)(CO) (7a).} Compound **6a** (0.100 g, 0.204 mmol) was taken into hexanes (5 mL) in a thick walled glass vessel fitted with a Kontes valve. The mixture was freeze-pump-thaw degassed three times using high vacuum. The headspace of the reaction vessel, frozen in liquid nitrogen, was backfilled with dihydrogen. The Kontes valve was sealed, and the reaction was allowed to warm to room temperature behind a blast shield. Upon warming to room temperature, the reaction gradually lightened in color. After 24 h, a pale red-yellow solution is observed. At this time, the reaction was refrozen in liquid nitrogen, and the hydrogen pressure was released by carefully opening the Kontes valve to a Schlenk line connected to a mercury bubbler. Hexanes were removed under vacuum, and a minimal amount of pentane was added to dissolve all of the solids. This mixture was stored at -35 °C overnight and generated small clusters of colorless crystals (yield, 0.046 g, 46%). ³¹P{¹H} NMR (C_6D_6 , 161.9 MHz, 298 K): δ 74.5 (d, $^2J_{PP} = 252.3$ Hz, 1P, Ru-PP^r₃), 92.9 (d, $^2J_{PP} = 252.3$ Hz, 1P, Ru-P_{ligand}). ¹H NMR (C_6D_6 , 400 MHz, 298 K): δ -18.4 (ddd, $^2J_{HH} = 6.7$ Hz, $^2J_{PH} = 18.4$ Hz, $^2J_{PH} = 28.8$ Hz, 1H, *trans*-N-Ru-H), -5.5 (ddd, $^2J_{HH} = 6.7$ Hz, $^2J_{PH} = 22.1$ Hz, $^2J_{PH} = 32.2$ Hz, 1H, *trans*-CO-Ru-H), 1.2 (m, 33H, N/P-PrⁱCH₃), 1.3 (d, $^3J_{HH} = 7.2$ Hz, 3H, N-PrⁱCH₃), 1.4 (d, $^3J_{HH} = 7.2$ Hz, 4H, N-PrⁱCH₂/ γ -CH₂), 1.4(6) (m, 1H, δ -CH₂), 1.6 (m, 4H, 2 \times β -CH₂/ δ -CH₂/ γ -CH₂), 1.7 (d, $^3J_{HH} = 6.6$ Hz, 3H, N-PrⁱCH₃), 1.9 (m, 2H, P-PrⁱCH₃), 2.0 (m, 3H, P-PrⁱCH₃), 3.0 (sept $^3J_{HH} = 6.72$ Hz, 1H, N-PrⁱCH), 3.2 (v dd, $J = 10.3$ Hz, $J = 20.1$ Hz, 1H, α -CH), 3.7 (sept. $^2J_{HH} = 6.76$ Hz, 1H, N-PrⁱCH), 7.0 (dd, $^4J_{HH} = 1.0$ Hz, $^3J_{HH} = 7.5$ Hz, 1H, N-*m*-ArCH), 7.1 (v t, $^3J_{HH} = 7.6$ Hz, 1H, N-*p*-ArCH), 7.1 (dd, $^4J_{HH} = 1.0$ Hz, $^3J_{HH} = 7.7$ Hz, 1H, N-*m*-ArCH). ¹³C APT NMR (C_6D_6 , 100.6 MHz, 298 K): δ 18.3 (d, $^2J_{PC} = 7.4$ Hz, P-PrⁱCH₃), 19.1 (d, $^2J_{PC} = 5.7$ Hz, P-PrⁱCH₃), 19.2 (s, P-PrⁱCH₃), 21.0 (m, P-PrⁱCH₃), 21.1 (d, $^2J_{PC} = 3.7$ Hz, P-PrⁱCH₃), 21.5 (d, $^2J_{PC} = 3.5$ Hz, P-PrⁱCH₃), 23.8 (dd, $^3J_{PC} = 2.4$ Hz, $^1J_{PC} = 11.5$ Hz, P-PrⁱCH), 24.2 (s, N-PrⁱCH₃), 24.7 (s, N-PrⁱCH₃), 25.2 (s, N-PrⁱCH₃), 25.5 (dd, $^4J_{PC} = 1.4$ Hz, $^3J_{PC} = 4.5$ Hz, δ -CH₂), 25.7 (s, N-PrⁱCH₃), 26.5 (dd, $^3J_{PC} = 2.7$ Hz, $^1J_{PC} = 16.7$ Hz, P-PrⁱCH), 26.9 (s, N-PrⁱCH), 27.4 (s, N-PrⁱCH), 27.6 (d, $^3J_{PC} = 4.2$ Hz, γ -CH₂), 31.2 (dd, $^3J_{PC} = 2.3$ Hz, $^1J_{PC} = 30.6$ Hz, P-PrⁱCH), 33.0 (d, $^2J_{PC} = 5.5$ Hz, β -CH₂), 55.7 (d, $^1J_{PC} = 11.0$ Hz, α -CH), 123.6 (s, N-*m*-ArCH), 125.1 (s, N-*p*-ArCH), 125.5 (s, N-*m*-ArCH), 137.8 (s, N-ArCPrⁱ), 139.2 (s, N-ArCPrⁱ), 150.7 (s, N-CAr), 193.5 (dd, $^3J_{PC} = 2.6$ Hz, $^2J_{PC} = 9.8$ Hz, N-C_{imine}), 208.9 (v t, $^3J_{PC} = 9.7$ Hz, Ru-CO). ATR-FTIR ν CO (cm⁻¹): 1881. Anal. Calcd for C₃₃H₆₁NOP₂Ru: C, 60.90; H, 9.45; N, 2.15. Found: C, 61.26; H, 9.52; N, 2.25.

General Procedure for Monitoring Formation of RuH₂^{[P^{ri}(NP)^{PrⁱH}](PP^r₃)(CO) (7a), RuH₂^{[Me(NP)^{PrⁱH}](PP^r₃)(CO) (7b), RuH₂^{[Me(NP)^{PrⁱH}](PP^r₃)(CO) (7c), and RuH₂^{[Me(NP)^{PrⁱH}](PP^r₃)(CO) (7d) under H₂.}}}} **6a**, **6b**, **6c**, or **6d** (0.031 mmol) was dissolved in *d*₈-toluene (0.50 mL) in a flame sealable NMR tube attached to a Kontes valve by a ground glass joint. The *d*₈-toluene contained 1,3,5-trimethoxybenzene as an internal standard. The mixture was freeze-pump-thaw degassed three times using high

vacuum. After this process, the tube was left submerged in liquid N₂, whereupon the headspace of the NMR tube was backfilled with H₂ to a total pressure of 38.0 mm Hg. The Kontes valve was sealed, and the NMR tube was flame-sealed such that 210 mm of headspace existed above the frozen toluene solution. The NMR tube was removed from liquid N₂ and allowed to warm to room temperature in a safe location. When the toluene solution melted, the time was recorded as the start of the reaction. After 30 min, a quantitative ¹H NMR spectrum was recorded. The tube was allowed to sit for 2 days, and then characterization by multinuclear NMR spectroscopy was performed.

RuH₂^{[P^{ri}(NP)^{PrⁱH}](PP^r₃)(CO) (7a).} The reaction is complete after 12 h using the above conditions. Multinuclear NMR data are reported above in the synthesis of **7a**.

RuH₂^{[Me(NP)^{PrⁱH}](PP^r₃)(CO) (7b).} After 2 days, two products are observed in a 2.4:1.0 ratio by ³¹P{¹H} NMR. The compound with $^2J_{PP} = 251.9$ Hz is present in higher concentration than the compound with $^2J_{PP} = 248.7$ Hz. ³¹P{¹H} NMR (*d*₈-toluene, 161.9 MHz, 298 K): δ 72.4 (d, $^2J_{PP} = 248.7$ Hz), 73.3 (d, $^2J_{PP} = 251.9$ Hz), 89.7 (d, $^2J_{PP} = 248.7$ Hz), 95.4 (d, $^2J_{PP} = 251.9$ Hz). ¹H NMR (*d*₈-toluene, 400 MHz, 298 K): Only resonances assigned to the major isomer are listed, all the resonances except for the hydrides were identified with the aid of a ¹H-¹³C HSQC NMR spectrum. There are many overlapping signals present. The data follow: δ -17.5 (ddd, $^2J_{HH} = 6.6$ Hz, $^2J_{PH} = 18.3$ Hz, $^2J_{PH} = 28.2$ Hz, 1H, *trans*-N-Ru-H), -5.6 (ddd, $^2J_{HH} = 6.8$ Hz, $^2J_{PH} = 21.5$ Hz, $^2J_{PH} = 31.9$ Hz, 1H, *trans*-CO-Ru-H), 1.3-1.5 (m, 21H, P-PrⁱCH₃), 1.5-1.6 (m, 11H, P-PrⁱCH₃, 2 \times β -CH₂), 1.6(3) (m, 2H, γ -CH₂/ δ -CH₂), 1.8 (m, 2H, γ -CH₂/ δ -CH₂), 2.0 (s, 3H, N-CH₃), 2.0(1)-2.2 (m, 5H, P-PrⁱCH), 2.6 (s, 3H, N-CH₃), 3.4 (dd, $J = 9.0$ Hz, $J = 20.3$ Hz, 1H, α -CH), 6.9-7.0 (m, 2H, N-ArCH), 7.1 (m, 1H, N-ArCH). ¹³C APT NMR (*d*₈-toluene, 100.6 MHz, 298 K): δ 18.1 (d, $^2J_{PC} = 7.5$ Hz, P-PrⁱCH₃), 18.3 (s, N-CH₃), 18.9 (s, N-CH₃), 19.4 (d, $^2J_{PC} = 4.3$ Hz, P-PrⁱCH₃), 20.7 (m, P-PrⁱCH₃, signal obscured by *d*₈-toluene CD₃ signal, identified by ¹H-¹³C HSQC), 20.9 (d, $^2J_{PC} = 2.8$ Hz, P-PrⁱCH₃), 21.1 (s, P-PrⁱCH₃), 21.4 (s, P-PrⁱCH₃), 23.7 (dd, $^3J_{PC} = 2.4$ Hz, $^1J_{PC} = 12.0$ Hz, P-PrⁱCH), 25.3 (v t, $^2J_{PC} = 6.8$ Hz, β -CH₂), 26.2 (d, $^1J_{PC} = 16.9$ Hz, P-PrⁱCH), 27.5 (d, $^3J_{PC} = 5$ Hz, γ -CH₂), 31.1 (dd, $^3J_{PC} = 2.1$ Hz, $^1J_{PC} = 24.3$ Hz, P-PrⁱCH), 35.3 (s, P-PrⁱCH), 55.2 (d, $^1J_{PC} = 11.9$ Hz, α -CH₂), 124.5 (s, N-ArCH), 127.9 (s, N-ArCH), 129.1 (s, N-ArCH), 152.1 (s, N-ArCCH₃), 191.3 (m, N-C_{imine}), 209.63 (m, Ru-CO). Resonances for N-CAr and N-ArCMe not observed, potentially due to poor S/N.

RuH₂^{[P^{ri}(NP)^{PrⁱH}](PP^r₃)(CO) (7c).} After 2 days, only signals assigned to the expected product could be detected by ¹H NMR spectroscopy. Allowing the reaction to proceed for 8 days gave approximately 40% conversion to **7c**. ³¹P{¹H} NMR (*d*₈-toluene, 161.9 MHz, 298 K): δ 76.0 (d, $^2J_{PP} = 251.5$ Hz, 1P, Ru-PP^r₃), 116.0 (d, $^2J_{PP} = 251.5$ Hz, 1P, Ru-P_{ligand}). ¹H NMR (*d*₈-toluene, 400 MHz, 298 K): δ -18.2 (ddd, $^2J_{HH} = 6.7$ Hz, $^2J_{PH} = 18.7$ Hz, $^2J_{PH} = 26.7$ Hz, 1H, *trans*-N-Ru-H), -5.7 (v dt, $^1J_{HH} = 6.7$ Hz, $^2J_{PH} = 25.4$ Hz, 1H, *trans*-CO-Ru-H).

RuH₂^{[Me(NP)^{PrⁱH}](PP^r₃)(CO) (7d).} After 2 days approximately 10% conversion is observed. Only one product is detected by ³¹P{¹H} NMR. The ¹H NMR spectrum shows a major and minor set of resonances corresponding to new products. The ratio between the major to the minor isomers is ~1:4. ³¹P{¹H} NMR (*d*₈-toluene, 161.9 MHz, 298 K): δ 74.0 (d, $^2J_{PP} = 250.8$ Hz, 1P, Ru-PP^r₃), 117.9 (d, $^2J_{PP} = 250.7$ Hz, 1P, Ru-P_{ligand}). ¹H NMR (*d*₈-toluene, 400 MHz, 298 K): δ -17.5 (ddd, $^2J_{HH} = 7.7$ Hz, $^2J_{PH} = 19.3$ Hz, $^2J_{PH} = 27.6$ Hz, 1H, Ru-H_{minor}), -17.3 (ddd, $^2J_{HH} = 7.0$ Hz, $^2J_{PH} = 19.0$ Hz, $^2J_{PH} = 27.0$ Hz, 1H, Ru-H_{major}), -14.7 (dd, $^2J_{PH} = 15.7$ Hz, $^2J_{PH} = 20.1$ Hz, 1H, Ru-H), -7.4 (br s, 4H, Ru-(H₂)(H)₂), -5.9 (m, 1H, Ru-H_{minor}), -5.8 (dd, $^2J_{HH} = 6.9$ Hz, $^2J_{PH} = 25.7$ Hz, 1H, Ru-H_{major}).

Formation of RuH₂(H₂)^{[P^{ri}(NP)^{PrⁱH}](PP^r₃)(CO) (8).} Reaction performed under H₂. Compound **6a** (0.020 g, 0.031 mmol) was dissolved in *d*₈-toluene (0.5 mL). This solution was transferred to a flame sealable NMR tube attached to a Kontes valve with a ground glass joint. The mixture was freeze-pump-thaw degassed three times using high vacuum and left submerged in liquid nitrogen. The headspace of the NMR tube was backfilled such that a meter stick attached to a column of mercury read 38.0 mm Hg. The Kontes valve was closed, and the

NMR tube was flame-sealed. The tube was removed from liquid nitrogen and allowed to warm to room temperature in a safe location. Within 20 min, the mixture mostly corresponds to **8**, such that meaningful multinuclear NMR spectra could be recorded. No attempts were made to isolate this intermediate as a pure solid. $^{31}\text{P}\{^1\text{H}\}$ NMR (C_6D_6 , 161.9 MHz, 298 K): δ 80.1 (d, $^2J_{\text{PP}} = 195.8$ Hz) and 41.2 (d, $^2J_{\text{PP}} = 195.8$ Hz). ^1H NMR (C_6D_6 , 400 MHz, 298 K): δ -7.2 (br s, 4H, $\text{Ru}-(\text{H}_2)\text{H}_2$), 1.0 (dd, $^3J_{\text{HH}} = 7.3$ Hz, $^3J_{\text{PH}} = 13.8$ Hz, 3H, $\text{P}-\text{Pr}^i\text{CH}_3$), 1.1 (dd, $^3J_{\text{HH}} = 7.1$ Hz, $^3J_{\text{PH}} = 13.4$ Hz, 18H, $\text{P}-\text{Pr}^i\text{CH}_3$), 1.2 (m, 12H, $\text{N}/\text{P}-\text{Pr}^i\text{CH}_3$), 1.3 (d, $^3J_{\text{HH}} = 6.8$ Hz, 3H, $\text{N}-\text{Pr}^i\text{CH}_3$), 1.3(s) (d, $^3J_{\text{HH}} = 6.8$ Hz, 3H, $\text{N}-\text{Pr}^i\text{CH}_3$), 1.4 (d, $^3J_{\text{HH}} = 6.8$ Hz, 3H, $\text{N}-\text{Pr}^i\text{CH}_3$), 1.5 (m, 2H, $\gamma\text{-CH}_2$), 1.9 (td, $^3J_{\text{HH}} = 6.8$ Hz, $^2J_{\text{PH}} = 13.8$ Hz, 3H, $\text{P}-\text{Pr}^i\text{CH}$), 2.0 (m, 1H, $\text{P}-\text{Pr}^i\text{CH}$), 2.1 (t, $^3J_{\text{HH}} = 7.3$ Hz, 2H, $\beta\text{-CH}_2$), 2.2 (td, $^3J_{\text{HH}} = 6.7$ Hz, $^3J_{\text{PH}} = 13.4$ Hz, 1H, $\text{P}-\text{Pr}^i\text{CH}$), 2.5 (t, $^3J_{\text{HH}} = 6.7$ Hz, 2H, $\delta\text{-CH}_2$), 3.6 (sept, $^3J_{\text{HH}} = 6.8$ Hz, 2H, $\text{N}-\text{Pr}^i\text{CH}$), 7.0(9) (m, 2H, $\text{N}-m\text{-ArCH}$), 7.1 (m, 1H, $\text{N}-p\text{-ArCH}$), 8.9 (s, 1H, $\text{N}_{\text{enamine}}\text{-H}$).

Formation of $\text{RuD}_2(\text{D}_2)\{\text{Pr}^i(\text{NP})\text{Pr}^i\text{D}\}(\text{PPR}^i_3)(\text{CO})$ (8**).** Reaction performed under D_2 . Similar conditions to those used to observe formation of $\text{RuH}_2(\text{H}_2)\{\text{Pr}^i(\text{NP})\text{Pr}^i\text{H}\}(\text{PPR}^i_3)(\text{CO})$ (**8**) were used. $^{31}\text{P}\{^1\text{H}\}$ NMR (C_6D_6 , 161.9 MHz, 298 K): No notable changes from reactions using H_2 are observed. ^1H NMR (C_6D_6 , 400 MHz, 298 K): The signals at δ -7.2 (br s, 4H, $\text{Ru}-(\text{H}_2)\text{H}_2$) and 8.9 (s, 1H, $\text{N}_{\text{enamine}}\text{-H}$) are changed from the spectrum recorded using H_2 gas. Integration of these resonances relative to a resonance at δ 2.5 (t, $^3J_{\text{HH}} = 6.7$ Hz, 2H, $\delta\text{-CH}_2$) that does not incorporate deuterium gives the ratio 11:1:75, $\text{Ru}-(\text{H}_2)\text{H}_2:\text{N}_{\text{enamine}}\text{-H}:\delta\text{-CH}_2$.

General Procedure for the Catalytic Dehydrogenation of Isopropanol to Acetone and Cyclohexanol to Cyclohexanone Using $\text{RuH}\{\text{Pr}^i(\text{NP})\text{Pr}^i\}(\text{PPR}^i_3)(\text{CO})$ (6a**).** A three neck flask (100 mL), fitted with a small stir bar and a reflux condenser connected to an Ar manifold vented to a mercury bubbler was used as the reaction vessel. In the glovebox, the three neck flask was charged with **6a** (0.040 g, 0.062 mmol) dissolved in toluene (2.00 mL). Using Schlenk techniques, the appropriate alcohol (6.2 mmol) was added. The three neck flask was lowered into a 60 °C oil bath and heated for approximately 12 h. After this period, the reaction mixture was sampled and analyzed by GC/MS. The trace showed complete consumption of isopropanol, and formation of acetone. By similar methods, it was determined approximately 50% of the cyclohexanol had been converted to cyclohexanone after 12 h.

Monitoring dehydrogenation of isopropanol to acetone by $\text{RuH}\{\text{Pr}^i(\text{NP})\text{Pr}^i\}(\text{PPR}^i_3)(\text{CO})$ (**6a**) by NMR. **6a** (0.020 g, 0.031 mmol) was dissolved in $d_8\text{-toluene}$ (0.5 mL) in a J. Young NMR tube. Isopropanol (0.024 mL, 0.31 mmol) was added to this mixture. The NMR tube was heated to 60 °C in the sealed tube overnight. Some conversion of isopropanol to acetone was detected under these conditions (3%). At room temperature, the headspace of the J. Young tube was evacuated. The J. Young tube was sealed under vacuum and lowered into a 60 °C oil bath for 2 h. More acetone formation was observed (5%). Monitoring the reaction while evacuating the headspace every hour showed an increase in percent conversion to acetone with time: 8% after 4 h to 9% after 9 h. The ratio between **6a**: **7a** varies but is approximately 1:1.2. The multinuclear NMR data reported below corresponds to the final reaction mixture. $^{31}\text{P}\{^1\text{H}\}$ NMR ($d_8\text{-toluene}$, 161.9 MHz, 298 K): δ -19.5 (s, 1P), 19.9 (s, 1P, PPR^i_3), 39.5 (d, $^2J_{\text{PP}} = 245.4$ Hz, 1P, $\text{Ru}-\text{PP}^i_{36a}$), 59.8 (d, $^2J_{\text{PP}} = 254.5$ Hz, 1P, $\text{Ru}-\text{P}_{\text{ligand}6a}$), 74.6 (d, $^2J_{\text{PP}} = 252.5$ Hz, 1P, $\text{P}-\text{RuPr}^i_{37a}$), 93.0 (d, $^2J_{\text{PP}} = 252.5$ Hz, 1P, $\text{Ru}-\text{P}_{\text{ligand}7a}$), 95.4 (s, 1P). ^1H NMR ($d_8\text{-toluene}$, 400 MHz, 298 K): δ -23.4 (t, $^2J_{\text{PH}} = 20.2$ Hz, $\text{Ru}-\text{H}_{6a}$), -18.6 (ddd, $^2J_{\text{HH}} = 6.6$ Hz, $^2J_{\text{PH}} = 18.3$ Hz, $^2J_{\text{PH}} = 25.5$ Hz, $\text{Ru}-\text{H}_{7a}$), -16.0 (d, $^3J_{\text{PH}} = 22.2$ Hz, $\text{Ru}-\text{H}$), -5.6 (ddd, $^2J_{\text{HH}} = 6.6$ Hz, $^2J_{\text{PH}} = 21.9$ Hz, $^2J_{\text{HH}} = 29.0$ Hz, $\text{Ru}-\text{H}_{7a}$), 1.0 (d, $^3J_{\text{HH}} = 6.1$ Hz, $\text{Pr}^i\text{OH}-\text{CH}_3$), 1.6 (s, acetone), 1.7 (s, $\text{Pr}^i\text{OH}-\text{OH}$), 3.7 (m, $\text{Pr}^i\text{OH}-\text{CH}$).

General Procedure for Attempted Catalytic Dehydrogenation of Benzyl Alcohol to Benzyl Benzoate Using $\text{RuH}\{\text{Pr}^i(\text{NP})\text{Pr}^i\}(\text{PPR}^i_3)(\text{CO})$ (6a**).** In the glovebox in a Schlenk flask (50 mL) fitted with a small stir bar, **6a** (0.020 g, 0.041 mmol) was dissolved in a 1.0 M solution of mesitylene in $d_8\text{-toluene}$ (2.0 mL). On the Schlenk line, benzyl alcohol (0.42 mL, 5 mmol) was added to the

mixture. The Schlenk flask was connected to a reflux condenser under a flow of Ar. The reaction vessel was lowered into a 60 °C oil bath. The reaction was vented to the Ar manifold of the Schlenk line, which was attached to a mercury bubbler. Before heating, and after 16 h, a small aliquot (0.5 mL) of the reaction mixture was sampled for analysis by NMR spectroscopy.

No Additive. Prior to heating, $^{31}\text{P}\{^1\text{H}\}$ NMR (C_6D_6 , 161.9 MHz, 298 K): δ 19.6 (s, $\text{P}-\text{Pr}^i_3$), 57.5 (s), 60.8 (s), 79.8 (s), 94.3 (s).

After heating to 60 °C, $^{31}\text{P}\{^1\text{H}\}$ NMR (C_6D_6 , 161.9 MHz, 298 K): δ 19.6 (s, $\text{P}-\text{Pr}^i_3$), 57.5 (s), 61.5 (s), 78.5 (d, $^2J_{\text{PP}} = 196.6$ Hz), 80.3 (d, $^2J_{\text{PP}} = 196.6$ Hz), 94.2 (s). ^1H NMR ($d_8\text{-toluene}$, 400 MHz, 298 K): δ -8.6 (td, $^3J_{\text{HH}} = 5.4$ Hz, $^2J_{\text{PH}} = 23.1$ Hz, $\text{Ru}-\text{H}$), -8.4 (td, $^2J_{\text{HH}} = 5.4$ Hz, $^2J_{\text{PH}} = 22.7$ Hz, $\text{Ru}-\text{H}$) 2.1 (s, *mesitylene*- CH_3), 3.3 (s, *benzyl alcohol*-OH), 4.3 (s, *benzyl alcohol*- CH_2), 5.0 (s, *benzyl benzoate*- CH_2), 6.6 (*mesitylene*-ArCH), 7.0-7.1 (ArCH). On the basis of integration of the CH_2 resonances of benzyl benzoate and benzyl alcohol, ~1% conversion occurred over 16 h.

Addition of PMe_3 . The conditions described above were repeated; however, PMe_3 (5 μL , 0.041 mmol) was added to the mixture of **6a** (0.020g, 0.041 mmol) dissolved in a 1.0 M solution of mesitylene in $d_8\text{-toluene}$ (2.0 mL).

Prior to heating to 60 °C, $^{31}\text{P}\{^1\text{H}\}$ NMR ($d_8\text{-toluene}$, 161.9 MHz, 298 K): δ 19.6 (s, $\text{P}-\text{Pr}^i_3$), 61.5 (s), 94.3 (s).

After heating to 60 °C, $^{31}\text{P}\{^1\text{H}\}$ NMR ($d_8\text{-toluene}$, 161.9 MHz, 298 K): δ 19.6 (s, $\text{P}-\text{Pr}^i_3$), 57.5 (s), 61.3 (s), 78.5 (d, $^2J_{\text{PP}} = 196.6$ Hz), 80.3 (d, $^2J_{\text{PP}} = 196.6$ Hz), 94.2 (s). ^1H NMR ($d_8\text{-toluene}$, 400 MHz, 298 K): δ -8.6 (td, $^2J_{\text{HH}} = 5.4$ Hz, $^2J_{\text{PH}} = 23.1$ Hz, $\text{Ru}-\text{H}$), -8.4 (td, $^2J_{\text{HH}} = 5.4$ Hz, $^2J_{\text{PH}} = 22.7$ Hz, $\text{Ru}-\text{H}$). Chemical shifts similar to those reported above for benzyl alcohol, benzyl benzoate, and mesitylene are observed here. On the basis of integration of the CH_2 resonances of benzyl benzoate and benzyl alcohol ~3% conversion has occurred over 16 h.

Addition of Pyridine. The conditions described above were repeated; however, pyridine (3.3 μL , 0.041 mmol) was added to the mixture of **6a** (0.020g, 0.041 mmol) dissolved in 1.0 M mesitylene in $d_8\text{-toluene}$ (2.0 mL).

Prior to heating to 60 °C, $^{31}\text{P}\{^1\text{H}\}$ NMR ($d_8\text{-toluene}$, 161.9 MHz, 298 K): δ 5.6 (s), 19.6 (s, $\text{P}-\text{Pr}^i_3$), 21.5 (s), 22.4 (s), 23.1 (s).

After heating to 60 °C, $^{31}\text{P}\{^1\text{H}\}$ NMR ($d_8\text{-toluene}$, 161.9 MHz, 298 K): δ 19.6 (s), 57.5 (s), 61.7 (s), 75.2 (s), 94.2 (s). ^1H NMR ($d_8\text{-toluene}$, 400 MHz, 298 K): Chemical shifts similar to those reported above for benzyl alcohol, benzyl benzoate, and mesitylene are observed here. On the basis of the integration of the CH_2 resonances of benzyl benzoate and benzyl alcohol ~2% conversion has occurred over 16 h.

■ ASSOCIATED CONTENT

📄 Supporting Information

Synthesis of the ligands including NMR data, summarized X-ray crystallographic, and IR spectral data. Crystallographic data are also provided in CIF format. The Supporting Information is available free of charge on the ACS Publications website at DOI: 10.1021/acs.inorgchem.5b00672.

■ AUTHOR INFORMATION

Corresponding Author

*E-mail: fryzuk@chem.ubc.ca.

Notes

The authors declare no competing financial interest.

■ ACKNOWLEDGMENTS

We thank NSERC of Canada for funding in the form of a Discovery Grant to M.D.F.

■ REFERENCES

- (1) Grützmacher, H. *Angew. Chem., Int. Ed.* **2008**, *47*, 1814.
- (2) Gunanathan, C.; Milstein, D. *Acc. Chem. Res.* **2011**, *44*, 588.
- (3) Gelman, D.; Musa, S. *ACS Catal.* **2012**, *2*, 2456.

- (4) Annibale, V. T.; Song, D. *RSC Adv.* **2013**, *3*, 11432.
- (5) Schneider, S.; Meiners, J.; Askevold, B. *Eur. J. Inorg. Chem.* **2012**, *2012*, 412.
- (6) Fryzuk, M. D.; MacNeil, P. A. *Organometallics* **1983**, *2*, 682.
- (7) Fryzuk, M. D.; MacNeil, P. A.; Rettig, S. J. *Organometallics* **1985**, *4*, 1145.
- (8) Fryzuk, M. D.; MacNeil, P. a.; Rettig, S. J. *J. Am. Chem. Soc.* **1987**, *109*, 2803.
- (9) Zhang, J.; Leitius, G.; Ben-David, Y.; Milstein, D. *Angew. Chem., Int. Ed.* **2006**, *45*, 1113.
- (10) Zhang, J.; Leitius, G.; Ben-David, Y.; Milstein, D. *J. Am. Chem. Soc.* **2005**, *127*, 10840.
- (11) Blum, Y.; Shvo, Y. *J. Organomet. Chem.* **1985**, *282*, C7.
- (12) Annibale, V. T.; Dalessandro, D. A.; Song, D. *J. Am. Chem. Soc.* **2013**, *135*, 16175.
- (13) Gunanathan, C.; Gnanaprakasam, B.; Iron, M. A.; Shimon, L. J. W.; Milstein, D. *J. Am. Chem. Soc.* **2010**, *132*, 14763.
- (14) Stepowska, E.; Jiang, H.; Song, D. *Chem. Commun.* **2010**, *46*, 556.
- (15) Zhang, J.; Gandelman, M.; Shimon, L. J. W.; Milstein, D. *Dalton Trans.* **2007**, 107.
- (16) Balaraman, E.; Fogler, E.; Milstein, D. *Chem. Commun.* **2012**, *48*, 1111.
- (17) Sun, Y.; Koehler, C.; Tan, R.; Annibale, V. T.; Song, D. *Chem. Commun.* **2011**, *47*, 8349.
- (18) Gargir, M.; Ben-David, Y.; Leitius, G.; Diskin-Posner, Y.; Shimon, L. J. W.; Milstein, D. *Organometallics* **2012**, *31*, 6207.
- (19) Ben-Ari, E.; Leitius, G.; Shimon, L. J. W.; Milstein, D. *J. Am. Chem. Soc.* **2006**, *128*, 15390.
- (20) Friedrich, A.; Drees, M.; Kass, M.; Herdtweck, E.; Schneider, S. *Inorg. Chem.* **2010**, *49*, 5482.
- (21) Huff, C. A.; Kampf, J. W.; Sanford, M. S. *Chem. Commun.* **2013**, *49*, 7147.
- (22) Huff, C. A.; Kampf, J. W.; Sanford, M. S. *Organometallics* **2012**, *31*, 4643.
- (23) Feller, M.; Diskin-Posner, Y.; Shimon, L. J. W.; Ben-Ari, E.; Milstein, D. *Organometallics* **2012**, *31*, 4083.
- (24) Montag, M.; Zhang, J.; Milstein, D. *J. Am. Chem. Soc.* **2012**, *134*, 10325.
- (25) Chang, Y.-H.; Nakajima, Y.; Tanaka, H.; Yoshizawa, K.; Ozawa, F. *Organometallics* **2014**, *33*, 715.
- (26) Schwartsburd, L.; Iron, M. a.; Konstantinovski, L.; Diskin-Posner, Y.; Leitius, G.; Shimon, L. J. W.; Milstein, D. *Organometallics* **2010**, *29*, 3817.
- (27) Li, H.; Wang, X.; Wen, M.; Wang, Z.-X. *Eur. J. Inorg. Chem.* **2012**, *2012*, 5011.
- (28) Hasanayn, F.; Baroudi, A.; Bengali, A. A.; Goldman, A. S. *Organometallics* **2013**, *32*, 6969.
- (29) Li, H.; Wen, M.; Wang, Z.-X. *Inorg. Chem.* **2012**, *51*, 5716.
- (30) Zeng, G.; Li, S. *Inorg. Chem.* **2011**, *50*, 10572.
- (31) Wambach, T. C.; Ahn, J. M.; Patrick, B. O.; Fryzuk, M. D. *Organometallics* **2013**, *32*, 4431.
- (32) Keim, W.; Killat, S.; Nobile, C. F.; Paolo, G.; Englert, U.; Wang, R.; Mecking, S.; Schroder, D. L. *J. Organomet. Chem.* **2002**, *662*, 150.
- (33) Guan, Z.; Marshall, W. J. *Organometallics* **2002**, *21*, 3580.
- (34) Zhu, T.; Wambach, T. C.; Fryzuk, M. D. *Inorg. Chem.* **2011**, *50*, 11212.
- (35) Riehl, J. F.; Jean, Y.; Eisenstein, O.; Pelissier, M. *Organometallics* **1992**, *11*, 729.
- (36) Käß, M.; Friedrich, A.; Drees, M.; Schneider, S. *Angew. Chem., Int. Ed.* **2009**, *48*, 905.
- (37) Friedrich, A.; Drees, M.; Schmedt auf der Günne, J.; Schneider, S. *J. Am. Chem. Soc.* **2009**, *131*, 17552.
- (38) Gusev, D. G.; Vymenits, A. B.; Bakhmutov, V. I. *Inorg. Chem.* **1992**, *31*, 1.
- (39) Bolton, P. D.; Grellier, M.; Vautravers, N.; Vendier, L.; Sabo-Etienne, S. *Organometallics* **2008**, *27*, 5088.
- (40) Jessop, P. G.; Morris, R. H. *Coord. Chem. Rev.* **1992**, *121*, 155.
- (41) Morris, R. H. *Coord. Chem. Rev.* **2008**, *252*, 2381.
- (42) Esteruelas, M. A.; Werner, H. J. *Organomet. Chem.* **1986**, *303*, 221.